Paradoxical activation and RAF inhibitor resistance of BRAF protein kinase fusions characterizing pediatric astrocytomas

Angela J. Sievert[a,b,1], Shih-Shan Lang[c,1], Katie L. Boucher[d], Peter J. Madsen[c,d], Erin Slaunwhite[d], Namrata Choudhari[d], Meghan Kellet[d], Phillip B. Storm[c,d], and Adam C. Resnick[c,d,2]

[a]Division of Oncology, The Children's Hospital of Philadelphia, Philadelphia, PA 19104; [b]Department of Pediatrics, Perelman School of Medicine at the University of Pennsylvania, Philadelphia, PA 19104; [c]Department of Neurosurgery, Perelman School of Medicine at the University of Pennsylvania, Philadelphia, PA 19104; and [d]Division of Neurosurgery, The Children's Hospital of Philadelphia, Philadelphia, PA 19104

Edited by Solomon H. Snyder, Johns Hopkins University School of Medicine, Baltimore, MD, and approved February 22, 2013 (received for review November 8, 2012)

Astrocytomas are the most common type of brain tumors in children. Activated BRAF protein kinase mutations are characteristic of pediatric astrocytomas with KIAA1549-BRAF fusion genes typifying low-grade astrocytomas and ^{V600E}BRAF alterations characterizing distinct or higher-grade tumors. Recently, BRAF-targeted therapies, such as vemurafenib, have shown great promise in treating V600E-dependent melanomas. Like ^{V600E}BRAF, BRAF fusion kinases activate MAPK signaling and are sufficient for malignant transformation; however, here we characterized the distinct mechanisms of action of KIAA1549-BRAF and its differential responsiveness to PLX4720, a first-generation BRAF inhibitor and research analog of vemurafenib. We found that in cells expressing KIAA1549-BRAF, the fusion kinase functions as a homodimer that is resistant to PLX4720 and accordingly is associated with CRAF-independent paradoxical activation of MAPK signaling. Mutagenesis studies demonstrated that KIAA1549-BRAF fusion-mediated signaling is diminished with disruption of the BRAF kinase dimer interface. In addition, the KIAA1549-BRAF fusion displays increased binding affinity to kinase suppressor of RAS (KSR), an RAF relative recently demonstrated to facilitate MEK phosphorylation by BRAF. Despite its resistance to PLX4720, the KIAA1549-BRAF fusion is responsive to a second-generation selective BRAF inhibitor that, unlike vemurafenib, does not induce activation of wild-type BRAF. Our data support the development of targeted treatment paradigms for BRAF-altered pediatric astrocytomas and also demonstrate that therapies must be tailored to the specific mutational context and distinct mechanisms of action of the mutant kinase.

targeted therapeutics | dimerization

Low-grade astrocytomas are the most common cancer of the central nervous system in children. They represent a heterogeneous group of tumors that can be found anywhere within the brain or spinal cord. Surgical resection may be curative; however, up to 20% of children suffer from progressive and/or disseminated tumor burden, which can result in significant morbidity and mortality (1). Treatment options are limited for children with recurrent and/or disseminated tumors, as well as those with tumors not amenable to surgical resection; thus, there is a significant unmet need for effective targeted therapeutics for children with unresectable or progressive astrocytomas.

The discovery of an oncogenic KIAA1549-BRAF fusion as a hallmark genetic event in pediatric low-grade astrocytomas suggests that recently developed targeted approaches may offer therapeutic opportunities for BRAF-altered tumors (2–4). The *KIAA1549-BRAF* fusion gene forms as a result of an internal, nonrandom tandem duplication event in chromosome 7q34 in which the N terminus of the KIAA1549 gene is fused with the C terminus of BRAF, preserving the BRAF kinase domain. The prevalence of this oncogenic KIAA1549-BRAF fusion gene and paucity of other common mutations suggest that the BRAF fusion alteration is a crucial initiating driving event in pediatric low-grade astrocytoma tumorigenesis.

The RAS/RAF/MEK/ERK mitogen-activated protein kinase (MAPK) cascade is one of the most extensively described and studied oncogenic signal transduction pathways. RAF kinases are activated upon association with receptor-activated RAS, and in turn phosphorylate and activate MEK1/2 and, consequently, the downstream targets ERK1/2 (5). Activating BRAF mutations occur in a number of non-central nervous system tumors, including primary melanomas, papillary thyroid carcinomas, and colorectal cancers (6). The vast majority (>90%) of BRAF mutations represent a single amino acid substitution of valine to glutamate in exon 15 at residue 600 (V600E) (6). Recently developed targeted therapies for BRAF-altered tumors have proven remarkably efficacious. RAF inhibitors, such as vemurafenib (PLX4032), display robust antitumor activity in ^{V600E}BRAF-positive melanomas, leading to accelerated Food and Drug Administration approval for use in metastatic or unresectable tumors. Vemurafenib displays selective, potent inhibition of ^{V600E}BRAF in mutant cells, but also can induce "paradoxical" activation of the MAPK pathway in cells expressing wild-type BRAF, particularly in the context of RAS activation or activated receptor tyrosine kinases (7).

Targeted inhibition of BRAF fusion proteins has not been described previously. In large part, this is likely the result of the failure to establish patient-derived model systems that harbor BRAF fusions. In order to characterize KIAA1549-BRAF fusion targeting by selective BRAF inhibition, we generated stably expressing BRAF fusion cell lines in a number of well-established systems, including NIH/3T3, Ba/F3, and primary mouse neurosphere cells. Here we characterize and molecularly define KIAA1549-BRAF fusion targeting in these stably expressing cell lines by PLX4720, the research analog of vemurafenib, and PLX PB-3, a recently developed second-generation BRAF inhibitor.

Results and Discussion

A number of different KIAA1549-BRAF fusion variants are found in patients with various elements of KIAA1549 fused to the kinase domain of BRAF (8). Recently, additional RAF fusions have been characterized in low-grade astrocytomas, including a 47-kDa family with sequence similarity 131, member B (FAM131B)-BRAF fusion (9). However, to our knowledge there are no established pediatric low-grade astrocytoma cell lines endogenously expressing BRAF fusions, and indeed very few available pediatric high-grade astrocytoma cell lines. To study KIAA1549-BRAF–mediated oncogenic signaling and molecular targeting, we generated four mutant fusion BRAF constructs (Fig. 1*A*). Two of these

Author contributions: A.J.S., S.-S.L., P.B.S., and A.C.R. designed research; A.J.S., S.-S.L., K.L.B., P.J.M., E.S., N.C., M.K., and A.C.R. performed research; A.J.S., S.-S.L., P.B.S., and A.C.R. analyzed data; and A.J.S., S.-S.L., and A.C.R. wrote the paper.

The authors declare no conflict of interest.

This article is a PNAS Direct Submission.

Freely available online through the PNAS open access option.

[1]A.J.S. and S.-S.L. contributed equally to this work.

[2]To whom correspondence should be addressed. E-mail: resnick@email.chop.edu.

This article contains supporting information online at www.pnas.org/lookup/suppl/doi:10.1073/pnas.1219232110/-/DCSupplemental.

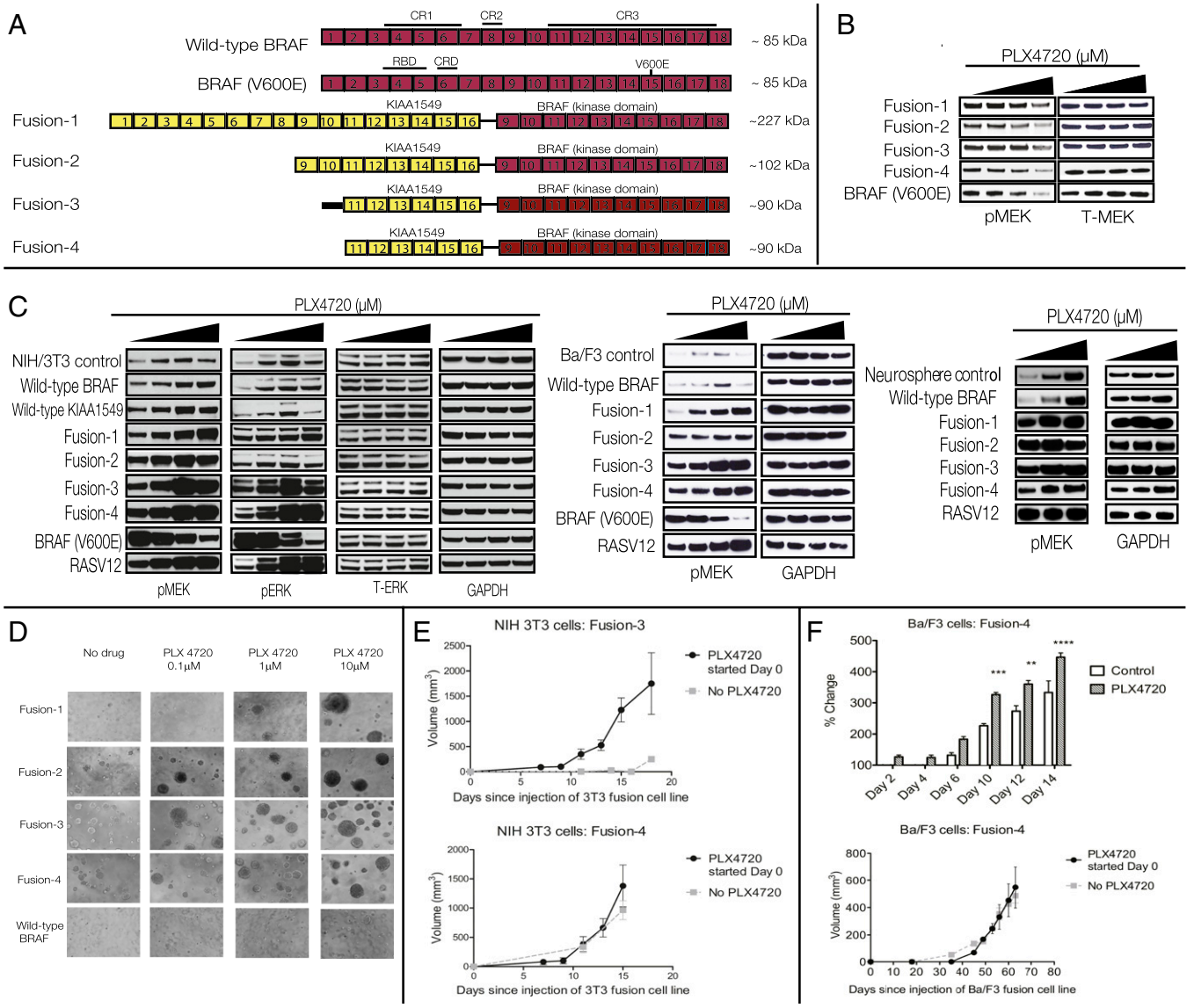

Fig. 1. Cells expressing KIAA1549-BRAF fusions display resistance and an associated enhanced paradoxical activation in response to first generation targeted BRAF inhibition. (*A*) KIAA1549-BRAF fusions are the result of an internal tandem duplication event that fuses KIAA1549, an uncharacterized gene, with the C terminus BRAF kinase domain (lacking the autoinhibitory N terminus). Constructs used in this study include Fusion-1 (long-form fusion protein), Fusion-2 (short-form fusion protein), and Fusion-3 and Fusion-4, proteins further truncated to eliminate putative KIAA1549 transmembrane domains, with Fusion-3 further modified to include an N terminus Src myristoylation sequence for membrane localization. Wild-type BRAF and ^{V600E}BRAF sequences are shown for comparison. CR1, conserved region 1; CR2, conserved region 2; CR3, conserved region 3; CRD, cystine-rich domain; RBD, RAS-binding domain. (*B*) BRAF fusion constructs demonstrate similar responses to targeted BRAF inhibition with PLX4720 in in vitro kinase assays. Myc-tagged ^{V600E}BRAF and KIAA1549-BRAF Fusion-1–Fusion-4 were transiently overexpressed in HEK293T cells. Kinases were immunoprecipitated, and in vitro kinase assays were performed with purified MEK in the presence of increasing concentrations of PLX4720 (0, 0.1,1, and 10 μM) over 30 min. The inhibitory effects of increasing concentrations of PLX4720 were evaluated by Western blot analysis using anti–phospho-MEK1/2. (*C*) Cell lines stably overexpressing the BRAF fusion constructs demonstrate resistance and enhanced paradoxical activation in the presence of targeted BRAF inhibition with PLX4720. The Western blots show MAPK pathway responsiveness in the presence of increasing concentrations (0, 0.01, 0.1, 1, and 10 μM) of PLX4720 in stably selected NIH/3T3 KIAA1549-BRAF cell lines (*Left*), Ba/F3 KIAA1549-BRAF cell lines (*Center*), and murine cortical neurosphere KIAA1549-BRAF cell lines (*Right*). As described previously for neurospheres, ^{V600E}BRAF-expressing cells entered senescence (26) and thus were excluded from this analysis. (*D*) NIH/3T3 cells stably expressing KIAA1549-BRAF Fusion-1–Fusion-4 display increased anchorage-independent cell growth in the presence of increasing concentrations of PLX4720 (0, 0.1, 1, and 10 μM) compared with cells expressing wild-type BRAF. (*E*) NIH/3T3 cells stably expressing KIAA1549-BRAF Fusion-3 (*Upper*) and Fusion-4 (*Lower*) cells demonstrate accelerated tumor growth in the presence of PLX4720. On the day of injection, mice were started on treatment with PLX4720-infused chow or received control chow. Both fusion cell lines were resistant to PLX4720. Data are mean ± SEM of five mice. The *y* axis shows tumor volume in cubic millimeters; *x* axis, days since injection. (*F*) Ba/F3 cells stably expressing KIAA-BRAF Fusion-4 demonstrate increased cell proliferation and accelerated tumor growth in the presence of PLX4720. (*Upper*) The IL-3–independent stably selected Ba/F3 Fusion-4 cell line demonstrates increased cell proliferation in the presence of PLX4720 (0.1 μM for 2 wk). Data are percent change in mean cell count ± SEM. (*Lower*) The Ba/F3 KIAA1549-BRAF Fusion-4 cell line was injected into the flanks of balb/c nu/nu mice. On the day of injection, mice were started on treatment with PLX4720-infused chow or received control chow. Results are comparable to those found with the NIH/3T3 KIAA1549-BRAF fusion cell lines, with the Ba/F3 Fusion-4 tumors demonstrating resistance to PLX4720. Data are mean ± SEM of five mice. The *y* axis shows tumor volume in cubic millimeters; the *x* axis, days since injection.

constructs, termed Fusion-1 and Fusion-2, recapitulate two forms of KIAA1549-BRAF genes found in patients. Fusion-1 represents a long, commonly expressed mutant that results from a KIAA1549 exon 16-BRAF exon 9 fusion event, and Fusion-2 is a shorter transcript of the fusion that forms as result of a KIAA1549 alternate start site in intron 8 (3). Independent of the cell lines tested, both Fusion-1 and Fusion-2 are expressed at significantly lower levels than comparable constructs of wild-type BRAF or ^{V600E}BRAF. To account for these expression differences, and to assess the contribution of KIAA1549 to KIAA1549-BRAF signaling, we also generated two additional constructs, termed Fusion-3 and Fusion-4, that further truncate the KIAA1549 N terminus just beyond two putative transmembrane domains. Fusion-3 incorporates an N-terminal myristoylation sequence to restore membrane localization to the protein. Intriguingly, although the recently identified FAM131B-BRAF fusion does not contain predicted transmembrane domains, like Fusion-3, it does contain an *N*-myristoylation motif (10), suggesting the potential selection for membrane-localized fusion partners of BRAF in gliomas. Using the KIAA1549-BRAF constructs, we generated and characterized stably expressing, virally transduced NIH/3T3, Ba/F3, and murine cortical neurosphere cell lines (Fig. S1 *A*–*E*).

We first assayed KIAA1549-BRAF fusion signaling and targeting biochemically after immunoprecipitation from overexpressing human embryonic kidney (HEK) 293T cells. Kinase assays demonstrated equal or greater in vitro activity for immunoprecipitated KIAA1549-BRAF fusions and ^{V600E}BRAF. Likewise, similar concentrations of PLX4720 inhibited in vitro phosphorylation of MEK1 by either ^{V600E}BRAF or KIAA1549-BRAF fusions (Fig. 1*B*). In contrast, cell lines stably expressing KIAA1549-BRAF constructs were resistant to PLX4720 inhibition and/or displayed enhanced "paradoxical" activation with increased phosphorylation of MEK and ERK1/2 in the presence of increasing concentrations of PLX4720 (Fig. 1*C*). Resistance and/or paradoxical activation was observed in all BRAF fusion-expressing cells; however, the degrees of activation or drug resistance at different drug concentrations differed, likely owing to the differences in the fusion constructs and their respective expression levels in the different cell lines. (A detailed description of each fusion construct is provided in *Methods*.) In these settings, membrane localization did not appear to impart distinct phenotypes, however. Taken together, these data show that under conditions of serum withdrawal in which paradoxical activation of wild-type BRAF is suppressed, KIAA1549-BRAF uniquely acts to consistently impart resistance and enhanced activation of the pathway in response to PLX4720.

Activator protein-1 (AP-1) promoter activity assays demonstrated similar results, with KIAA1549-mediated activation of the AP-1 promoter showing enhanced activation in the presence of drug (Fig. S2*A*). The observed KIAA1549-BRAF–mediated resistance and enhanced MAPK activation were complemented by MAPK-dependent cellular phenotypes in the respective cell lines. Anchorage-independent growth of transformed KIAA1549-BRAF fusion expressing NIH/3T3 cells was either unaffected or increased in the presence of increasing concentrations of PLX4720 (Fig. 1*D*). Similarly, NIH/3T3 cells expressing KIAA1549-BRAF also displayed resistance and/or increased tumor growth in vivo when injected into the flank of immunocompromised balb/c nu/nu mice maximally dosed with PLX4720 (Fig. 1*E* and Fig. S2*C*). Ba/F3 cells require IL-3 for growth, but this dependence can be overcome by constitutive MAPK activation (11). Previous studies have demonstrated that Ba/F3 cells can be rendered IL-3–independent upon ^{V600E}BRAF expression, but not wild-type BRAF expression (12). Accordingly, we were able to demonstrate IL-3 independence in Ba/F3 cells stably expressing the KIAA1549-BRAF fusion constructs (Fig. S2*B*). In response to PLX4720 administration, IL-3–independent proliferation rates of KIAA1549-BRAF fusion harboring Ba/F3 cells failed to slow and actually increased, complementing the enhanced phosphorylated MEK observed in the presence of drug, and, like the NIH/3T3 cells, failed to respond to PLX4720 in mouse flank models (Fig. 1*F* and Fig. S2*C*).

In normal or cancerous cells harboring wild-type BRAF, selective BRAF inhibitors, including vemurafenib, can induce activation of the MAPK pathway, particularly in the context of mutated or activated RAS. Vemurafenib promotes heterodimerization of wild-type BRAF with CRAF and at limiting concentrations induces transactivation of the non–drug-bound protomer by the drug-bound partner (7). We wondered whether similar dependencies mediate BRAF targeting resistance and enhanced paradoxical activation of the MAPK pathway in KIAA1549-BRAF–expressing cells. In contrast to the previously described role for CRAF in heterodimerization-dependent paradoxical activation of wild-type BRAF (7), RNA interference knockdown of CRAF in KIAA1549-BRAF expressing cells failed to alter PLX4720-induced phosphorylation of MEK1/2 (Fig. 2*A*). This finding suggests that CRAF is dispensable for the drug resistance and/or induced activation observed in BRAF fusion-expressing cells.

RAF dimerization and activation are negatively regulated by the proteins' RAS-binding amino terminus (13). Loss or truncation of the N terminus regulatory domain results in the RAS-independent, constitutive dimerization of RAFs. To assess homodimerization and heterodimerization of KIAA1549-BRAF fusions, we transiently cooverexpressed differentially tagged (GST or Myc) wild-type, V600E, and KIAA1549-BRAF fusion constructs in NIH/3T3 cells and performed pull-down experiments. GST pull-

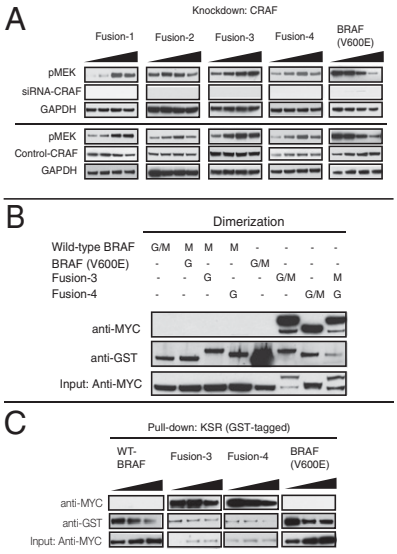

Fig. 2. BRAF fusions function as distinct, altered signaling complexes. (*A*) CRAF is dispensable for drug resistance and associated paradoxical activation in KIAA1549-BRAF fusion-expressing cells. Using RNA interference, CRAF was knocked down in NIH/3T3 BRAF cell lines stably expressing KIAA1549-BRAF fusions, and the effects of increasing concentrations of PLX4720 (0, 0.1, 1, and 10 μM) were evaluated by Western blot analysis. No change in paradoxical activation as evaluated by pMEK immunoblotting was seen in the NIH/3T3 cells expressing fusion constructs. (*B*) KIAA1549-BRAF fusions signal as constitutive homodimers. To compare levels of kinase dimerization, GST pull-downs were performed from NIH/3T3 cells combinatorially coexpressing Myc-tagged and GST-tagged wild-type BRAF, ^{V600E}BRAF, and indicated KIAA1549-BRAF fusions. Western blot analysis with anti-Myc or anti-GST antibodies was performed as indicated. Robust fusion–fusion homodimerization is evident with no evidence for fusion heterodimerization with wild-type BRAF or homodimerization of ^{V600E}BRAF. G, GST-tagged constructs; M, Myc-tagged constructs. (*C*) KIAA1549-BRAF fusions display enhanced interactions with KSR1. Stably selected NIH/3T3 KIAA1549-BRAF cell lines expressing Myc-tagged wild-type BRAF, Fusion-3, Fusion-4, and ^{V600E}BRAF constructs were transfected with GST-KSR1 and incubated with increasing concentrations of PLX4720 (0, 1, and 10 μM). GST pull-downs were performed, and protein interactions were assessed by Western blot analysis. KSR-1 displayed enhanced affinity for Fusion-3 and Fusion-4 compared with wild-type BRAF or ^{V600E}BRAF.

downs were immunoblotted for the associated Myc-tagged protein to assess the overexpressed proteins' homodimerization or heterodimerization. Although neither wild-type BRAF nor ^{V600E}BRAF displayed significant homodimerization or heterodimerization, KIAA1549-BRAF fusion proteins underwent robust, constitutive homodimerization independent of cell surface receptor activation (Fig. 2*B*).

Recently, a more prominent role for kinase suppressor of RAS (KSR) in regulating RAF phosphorylation of MEK that also implicates KSR-BRAF heterodimerization has been suggested (14). Furthermore, in a separate study, KSR1 was proposed to compete with CRAF for inhibitor-induced binding to BRAF and alter paradoxical activation induced by BRAF inhibition (15, 16). Although CRAF does not appear to play a role in the drug resistance or paradoxical activation associated with KIAA1549-BRAF signaling, we tested whether the fusion kinase displays altered or differential interactions with KSR1. Remarkably, whereas KIAA1549-BRAF fusion proteins did not display significant heterodimerization with nonfusion BRAFs, pull-down assays of co-overexpressed proteins demonstrated enhanced, preferential interactions between KSR1 and KIAA1549-BRAF. This finding is in stark contrast with KSR1's minimal association with ^{V600E}BRAF or wild-type BRAF (Fig. 2*C*). Thus, the KIAA1549-BRAF fusion protein appears to induce a distinctly altered protein–protein interaction context that may underlie its resistance to PLX4720 and the enhanced propensity for paradoxical activation of MAPK signaling in BRAF fusion-expressing cells.

In addition, recent studies using neurospheres expressing KIAA1549-BRAF have suggested the involvement of tuberin/RAS homolog enriched in brain (RHEB)-mediated mammalian target of rapamycin (mTOR) signaling in BRAF fusion signaling (17). We wondered whether mTOR signaling is also involved in the resistance and paradoxical activation phenotypes that we observed in the presence of PLX4720. In response to the drug, fold changes in phospho-AKT (Ser473) were largely similar across cell lines and did not correlate with increased MEK phosphorylation; similarly, proline-rich Akt/PKB substrate 40 kDa (PRAS40) (Ser183) phosphorylation did not correlate with paradoxical activation. In contrast, increasing concentrations of PLX4720 dramatically induced S6 phosphorylation in fusion-expressing cells, suggesting a possible role for mTOR signaling integration in drug resistance associated with KIAA1549-BRAF (Fig. S2*F*).

In normal cells, wild-type BRAF requires activated RAS to localize to the membrane, and upon RAS binding undergoes homodimerization or heterodimerization to activate MAPK signaling (13). To directly evaluate the role of dimerization in BRAF fusion signaling, we generated point mutant constructs in the putative dimerization interface of KIAA1549-BRAF corresponding to an arginine residue previously demonstrated to reduce wild-type BRAF dimerization when mutated to histidine (R509H) (18–20). Pull-down assays from NIH/3T3 cells coexpressing differentially tagged Fusion-3 and Fusion-4 demonstrated that the R509H mutation imparts a loss of dimerization potential to KIAA1549-BRAF fusions (Fig. 3*A*). In vitro kinase assays demonstrated a reduction in MEK phosphorylation capacity for R509H mutant fusions (Fig. S2*E*). Accordingly, NIH/3T3 cells stably expressing R509H mutant versions of KIAA1549-BRAF did not exhibit paradoxical MAPK activation or resistance to PLX4720 (Fig. 3*B*). Indeed, the R509H mutation significantly diminished the NIH/3T3 cell transformation capacity of BRAF fusions (Fig. 3*C*). R509H mutant cells also exhibited no anchorage-independent growth in soft agar assays (Fig. 3*C*), and either no capacity or reduced capacity to grow as flank-injected tumors in immunocompromised mice (Fig. 3*D*).

Recently, melanoma cells and patient-derived tumors with emergent resistance to vemurafenib were found to express a truncated p61BRAF(V600E) alternate splice variant that lacks exons 4–8 and exhibits enhanced homodimerization (19). Similarly, our data demonstrate that KIAA1549-BRAF fusion functions as a constitutive homodimer independent of RAS, suggesting a shared mechanism of resistance mediated by RAF dimerization associated with loss of the BRAF regulatory N terminus and RAS-binding domain. Resistance and/or increased paradoxical activation also may be affected by KIAA1549-BRAF/KSR heterodimerization. Whether a similar KSR interaction occurs in the p61BRAF(V600E) context is unknown.

In wild-type BRAF-expressing cells, first-generation BRAF inhibitors can enhance MAPK activation via paradoxical activation mechanisms that increase RAF dimerization and induce kinase transactivation. In contrast, in cells with low RAS-GTP expression, ^{V600E}BRAF signals as a monomer in a RAS-independent fashion and is exquisitely sensitive to inhibitors, such as vemurafenib (7, 21,

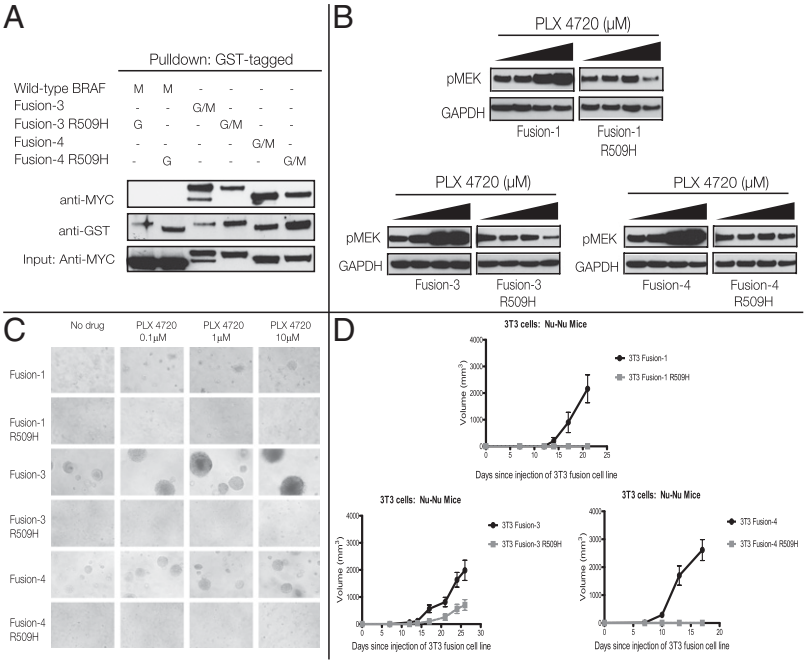

Fig. 3. BRAF fusion signaling is impaired by disruption of the dimerization interface. (*A*) Dimerization interface mutation impairs BRAF fusion homodimerization. To compare levels of kinase dimerization, GST pull-downs were performed from lysates of NIH/3T3 cells combinatorially coexpressing Myc-tagged and GST-tagged constructs. Robust fusion–fusion homodimerization was evident, but this dimerization was impaired when the R509H mutant was coexpressed. G, GST-tagged constructs; M, Myc-tagged constructs. (*B*) R509H mutant BRAF fusion constructs fail to demonstrate enhanced activation in response to PLX4720. MEK phosphorylation was assessed in NIH/3T3 cells stably expressing KIAA1549-BRAF fusions and the corresponding R509H mutants after incubation with increasing concentrations (0, 0.1, 1, and 10 μM) of PLX4720 for 30 min. (*C*) NIH/3T3 cells stably expressing KIAA1549-BRAF fusion R509H mutants display reduced transforming potential, associated with decreased anchorage-independent cell growth, and do not exhibit enhanced growth in the presence of increasing concentrations of PLX4720 (0, 0.1, 1, and 10 μM). (*D*) Disruption of the dimerization interface with a R509H mutation results in impaired tumor growth in vivo. NIH/3T3 cells stably expressing KIAA1549-BRAF fusions or the corresponding R509H mutants were injected into the flank of balb/c nu/nu mice. Data are mean ± SEM of five mice. The *y* axis indicates tumor volume in cubic millimeters; the *x* axis, days since injection.

22). Our data confirm that RAF dimerization underlies molecular mechanisms for both resistance and paradoxical activation in response to first-generation BRAF inhibitors. Recently, second-generation "paradox-breaking" BRAF inhibitors have been developed that retain selectivity and potency, but have a reduced capacity for activating wild-type BRAF. These compounds were developed by selecting for potency to block ^{V600E}BRAF-driven ERK phosphorylation while leaving RAS mutant ERK phosphorylation intact. PLX PB-3 is one such second-generation, selective RAF inhibitor. Like vemurafenib, PLX PB-3 displays modest selectivity for ^{V600E}BRAF over wild-type BRAF or CRAF, with respective IC_{50} values of 2.4 nM, 15 nM, and 21 nM. However, cell-based studies evaluating MAPK activation in HRAS mutant and ^{V600E}BRAF mutant cells suggest distinct pharmacologic profiles. Whereas both vemurafenib and PLX PB-3 display nearly identical, potent inhibition of phospho-ERK (pERK) in ^{V600E}BRAF-mutant cells, the well-described paradoxical activation associated with mutant RAS expression under vemurafenib treatment is absent upon treatment with PLX PB-3. We tested whether second-generation BRAF inhibitors such as PLX PB-3 could also overcome dimerization-dependent resistance and/or the enhanced paradoxical activation associated with the KIAA1549-BRAF fusion. Like PLX4720, PLX PB-3 equally inhibited both ^{V600E}BRAF and KIAA1549-BRAF in kinase reactions performed in vitro on immunoprecipitated enzymes expressed in HEK293T cells (Fig. 4*A*); however, in contrast to PLX4720, PLX PB-3 robustly inhibited KIAA1549-BRAF signaling and induced little to no paradoxical MAPK activation in BRAF fusion-expressing cells (Fig. 4*B*). PLX PB-3 also inhibited anchorage-independent growth of transformed NIH/3T3 cells expressing KIAA1549-BRAF fusion constructs (Fig. 4*C*). Similarly, in the presence of increasing concentrations of PLX PB-3, KIAA1549-BRAF fusion expressing Ba/F3 cells exhibited decreasing IL-3–independent proliferation rates (Fig. 4*D*). Inhibition of KIAA1549-BRAF–mediated signaling by PLX PB-3 did not appear to alter homodimerization, considering that similar protein–protein interactions were observed in the presence and absence of the drug (Fig. S2*D*).

How might second-generation BRAF inhibitors overcome resistance? The transactivation in the wild-type BRAF setting and the drug resistance observed in the KIAA1549-BRAF fusion constitutive homodimerization setting likely share mechanisms of allosteric modulation that result in enhanced kinase activity and reduced affinity for first-generation BRAF inhibitors. In contrast, and consistent with their reduced capacity for paradoxical activation, second-generation inhibitors, such as PLX PB-3, appear to inhibit both the ^{V600E}BRAF monomer and the KIAA1549-BRAF fusion constitutive dimer equally well, suggesting a similar capacity for inhibition in either a monomer or dimer setting. This model predicts that second-generation BRAF inhibitors, such as PLX PB-3, also may be capable of overcoming the p61BRAF (V600E)-mediated drug resistance observed in melanomas.

In conclusion, our data suggest that first-generation BRAF inhibitors, such as vemurafenib, are unlikely to be effective for single-agent treatment of astrocytomas expressing KIAA1549-BRAF fusion, and indeed may be contraindicated for these tumors. ^{V600E}BRAF alterations do occur in other low- and higher-grade histopathologies, suggesting that these tumors could potentially benefit from currently available BRAF-specific inhibitors, depending on the level of RAS activation present in these cells; however, additional studies are needed to assess the blood–brain barrier penetration of these compounds. Recent studies in patients with metastatic ^{V600E}BRAF-postive melanomas in the brain have suggested that MAPK-targeted approaches may indeed hold promise for brain tumors (23). In addition to FAM131B-BRAF, BRAF fusions involving genes other than KIAA1549 have been reported in other, nonastrocytoma tumor types, including thyroid, prostate, and gastric malignancies, in which BRAF is fused to A-kinase anchor protein 9 (AKAP9), solute carrier family 45, member 3 (SLC45A3), and type-1 angiotensin II receptor-associated protein (AGTRAP), respectively (24, 25). It is highly likely that all fusion kinases with BRAF truncations of the N terminus function as constitutive dimers and are resistant to current first-generation BRAF inhibitors, such as vemurafenib. Our demonstration that second-generation BRAF inhibitors, such as PLX PB-3, can successfully target KIAA1549-BRAF fusions characterizing pediatric astrocytomas provides support for new therapeutic opportunities for this class of BRAF-altered tumors.

Methods

Vector Construction and Generation of Stable Cell Lines. Unless indicated otherwise, full-length human gateway entry clones were purchased from Open Biosystems. A partial KIAA1549 (pF1KA1549) clone was purchased from Kazusa DNA Research Institute. Full-length KIAA1549 corresponding to NM_020910.1 was generated by extension PCR. Gateway cloning (Invitrogen) and site-directed mutagenesis were used to generate the following Myc-tagged constructs: wild-type BRAF, kinase-dead ^{K482M}BRAF mutant (KD), BRAF V600E mutant (V600E), HRASV12 mutant (RASV12), and wild-type KIAA1549. Full-length, "long form" KIAA1549-BRAF fusion (Fusion-1) was generated by translationally silent site-directed mutagenesis, providing restriction sites that permitted the construction of the KIAA1549-BRAF gene fusion via restriction digest/subcloning of the N terminus of KIAA1549 (exons 1–16) and the C

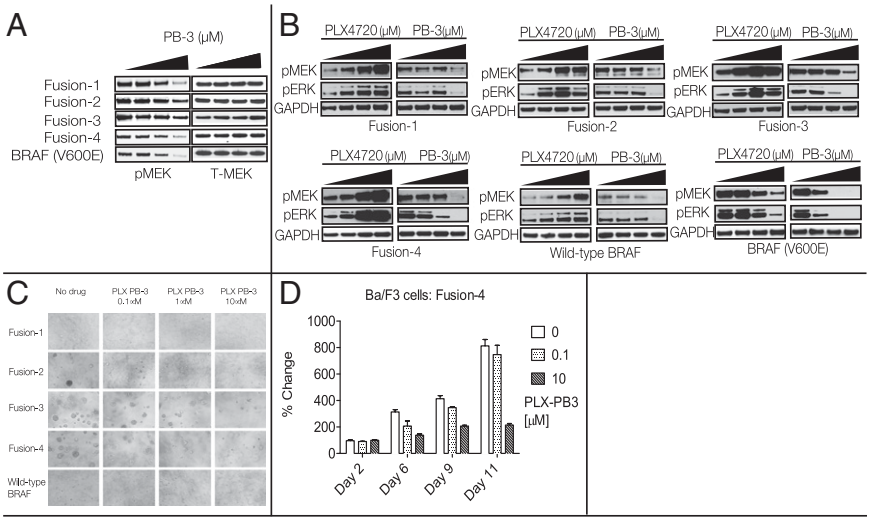

Fig. 4. BRAF fusion targeting by second-generation BRAF inhibitors. (*A*) BRAF fusion constructs demonstrate similar responses to selective BRAF inhibition with PLX PB-3 in in vitro kinase assays. Myc-tagged ^{V600E}BRAF and KIAA1549-BRAF Fusion 1–Fusion 4 were transiently overexpressed in HEK293T cells. Kinases were immunoprecipitated, and in vitro kinase assays were performed with purified MEK in the presence of increasing concentrations of PLX PB-3 (0, 0.1,1, and 10 μM) over 30 min. The effects of increasing concentrations of PLX PB-3 were analyzed by pMEK and total MEK (T-MEK) immunoblotting. (*B*) PLX PB-3 demonstrates abrogation of anti–phospho-MEK1/2 and ERK1/2 in all NIH/3T3 BRAF stably expressing cells. This is in contrast to the paradoxical activation and resistance seen with PLX4720 (Fig. 1*C*). (*C*) NIH/3T3 stably expressing KIAA1549-BRAF Fusion 1–Fusion 4 constructs display decreased anchorage-independent cell matrices in the presence of increasing concentrations of PLX PB-3 (0, 0.1, 1, and 10 μM). (*D*) IL-3–independent Ba/F3 cells stably expressing KIAA1549-BRAF fusions display decreased cell proliferation when incubated with PLX PB-3 (0.1 and 10 μM) for 2 wk. The decreased cell proliferation of Fusion-4 is in contrast to the increased cell proliferation seen in PLX4720-treated cells expressing Fusion-4 (Fig. 1*F*). Data are percent change of mean ± SEM.

terminus of BRAF (exons 9–18). A short form of the KIAA1549-BRAF fusion (Fusion-2), along with two different forms of the fusion that truncate the KIAA1549 C terminus immediately beyond the two putative transmembrane domains (predicted by TMHMM Server version 2.0) in KIAA1549 (Fusion-3 and Fusion-4), were generated via PCR using Fusion-1 as a template. The long form (Fusion-1) and short form (Fusion-2) KIAA1549-BRAF fusions are found in human tumors (pediatric low-grade astrocytomas). Fusion-3 and Fusion-4 were generated to enhance protein expression (see below).

Fusion-3 incorporates an N-terminal Src myristoylation sequence that permitted evaluation for the potential membrane targeting requirements of KIAA1549-BRAF; although membrane localization did not appear to substantially alter phenotypes associated with the mutant kinases. R509H mutants were also generated from each BRAF fusion construct via site-directed mutagenesis, as described above. Arginine 509 corresponds to the amino acid numbering associated with wild-type BRAF. To create stable NIH/3T3, Ba/F3, and neurosphere cell lines, the BRAF constructs were subcloned into a Gateway-compatible pMXs-Puro Retroviral Vector (Cell Biolabs). Retrovirus was produced using the Platinum-E retroviral packaging system (Cell Biolabs). Cells were infected with retrovirus in accordance with the manufacturer's suggested protocol and then selected for stable expression with puromycin. Stable, Myc-tagged protein expression was confirmed by Western blot analysis (Fig. S1 *A*–*C*). Fusion-1 and Fusion-2 displayed significantly lower expression levels than wild-type or ^{V600E}BRAF.

To ensure that differential RAF targeting or signaling was not the result of lower expression levels, we generated two additional fusion constructs, Fusion-3 and Fusion-4, and found that they had similar expression levels while retaining the signaling properties of full-length KIAA1549-BRAF. In stable NIH/3T3 cells, KIAA1549-BRAF displayed similar cell transformation and anchorage-independent growth as V600E- and activated RAS-expressing cells. In contrast, wild-type BRAF, kinase-dead ^{K482M}BRAF, and full-length KIAA1549 failed to transform cells and displayed identical behavior to untransformed NIH/3T3 cells (Fig. S1*D*). MAPK activation and serum responsiveness after 18 h of serum starvation were also characterized across the cell lines (Fig. S1*E*).

Cellular Transformation Assays. The ability of the BRAF mutants to transform cells by anchorage-independent growth was determined in a soft agar assay. Relative fluorescence units (RFU) from the assay were measured using the CytoSelect 96-Well Cell Transformation Assay (Cell Biolabs) in accordance with the manufacturer's recommendations.

Kinase Inhibition Studies. Selective BRAF inhibition studies were performed using a B-Raf Kinase Cascade Assay Kit (Millipore) in the presence of increasing concentrations of PLX4720, a first-generation BRAF-specific inhibitor, or PLX PB-3, a second-generation paradox-breaking BRAF-specific inhibitor (Plexxikon). Drug aliquots were dissolved in DMSO and stored at −20 °C. For BRAF inhibitor studies, cells were seeded in six-well dishes on the day before drug treatment, and the medium was changed to serum-free medium overnight. Drugs were added as indicated.

Animal Studies. PLX4720 inhibition studies were performed in a xenograft mouse model by injecting the fusion-harboring cell lines s.c. into the flanks of balb/c nu/nu mice maximally dosed with PLX4720 (PLX4720-containing chow, provided by Plexxikon). Tumor growth was measured with calipers on a bi-weekly basis. Ellipsoid tumor volume was calculated using the following formula: volume = 1/2·length·width^2.

Protein–Protein Interaction Assays. BRAF dimerization and KSR interactions studies were performed after transfection of HEK293T or NIH/3T3 using Lipofectamine LTX (Invitrogen). Immunoprecipitations (Myc) or pull-downs (GST) were performed at 4 °C for 4 h, followed by four washes with modified RIPA lysis buffer (50 mM Tris, 150 mM NaCl, 0.1% SDS, 0.5% sodium deoxycholate, 1% Nonidet P-40, Roche complete protease inhibitor mixture tablets, and 100× Pierce phosphatase inhibitor mixture) and a final wash with PBS.

Western Blot Analysis. Samples were normalized using a Pierce 660-nm Protein Assay and run on NuPAGE precast gels (4–12% Bis-Tris or Tris-acetate; Life Technologies). Blots were immunoblotted with the indicated primary antibodies: p217/p221-MEK (pERK; Cell Signaling), phospho-p44/42 MAPK (Thr202/Tyr204), pERK (Cell Signaling), Myc-Tag 9B11 (Cell Signaling), phospho-Akt (Ser473) (Cell Signaling), phospho-PRAS40 (Ser183) (Cell Signaling), phospho-S6 ribosomal protein (Ser235/236) (Cell Signaling), anti–c-Raf (BD Transduction Laboratories), anti-ERK1/2 (Promega), HRP-conjugated β-actin (Cell Signaling), and HRP-conjugated GAPDH (Cell Signaling). In some cases, proteins were detected with the Odyssey Imaging System (Li-Cor Biosciences).

AP-1 Promoter Activity and WST-1 Assays. Activity assays were performed using a Cignal AP1 Reporter (luc) Kit (Qiagen) and a Cell Proliferation WST-1 Kit (Roche) in accordance with the manufacturers' suggested protocols.

ACKNOWLEDGMENTS. We thank Plexxikon, Inc. for providing the PLX4720 and PB-3 compounds, Eric Raabe (Eberhart Lab, Johns Hopkins University) for providing the murine neurosphere cell lines, and John Maris and Gideon Bollag for discussing and reviewing the manuscript. This work was funded by the Matthew Larson Pediatric Brain Tumor Foundation (A.J.S.), an Alex's Lemonade Stand Young Investigator Award (to A.J.S.), the Rally Foundation for Childhood Cancer Research (A.J.S., S.-S.L., and A.C.R.), A Kid's Brain Tumor Cure/PLGA Foundation (A.C.R.), and the National Institutes of Health (Grant K12 CA076931, to A.J.S.; and Grant 5T32043126-09, to S.-S.L.).

1. Sievert AJ, Fisher MJ (2009) Pediatric low-grade gliomas. *J Child Neurol* 24(11):1397–1408.
2. Sievert AJ, et al. (2009) Duplication of 7q34 in pediatric low-grade astrocytomas detected by high-density single-nucleotide polymorphism-based genotype arrays results in a novel BRAF fusion gene. *Brain Pathol* 19(3):449–458.
3. Jones DT, et al. (2008) Tandem duplication producing a novel oncogenic BRAF fusion gene defines the majority of pilocytic astrocytomas. *Cancer Res* 68(21):8673–8677.
4. Lin A, et al. (2012) BRAF alterations in primary glial and glioneuronal neoplasms of the central nervous system with identification of 2 novel KIAA1549:BRAF fusion variants. *J Neuropathol Exp Neurol* 71(1):66–72.
5. Montagut C, Settleman J (2009) Targeting the RAF-MEK-ERK pathway in cancer therapy. *Cancer Lett* 283(2):125–134.
6. Davies H, et al. (2002) Mutations of the BRAF gene in human cancer. *Nature* 417(6892):949–954.
7. Poulikakos PI, Zhang C, Bollag G, Shokat KM, Rosen N (2010) RAF inhibitors transactivate RAF dimers and ERK signalling in cells with wild-type BRAF. *Nature* 464(7287):427–430.
8. Hasselblatt M, et al. (2011) BRAF-KIAA1549 fusion transcripts are less frequent in pilocytic astrocytomas diagnosed in adults. *Neuropathol Appl Neurobiol* 37(7):803–806.
9. Cin H, et al. (2011) Oncogenic FAM131B-BRAF fusion resulting from 7q34 deletion comprises an alternative mechanism of MAPK pathway activation in pilocytic astrocytoma. *Acta Neuropathol* 121(6):763–774.
10. Moriya K, et al. (2012) Protein N-myristoylation is required for cellular morphological changes induced by two formin family proteins, FMNL2 and FMNL3. *Biosci Biotechnol Biochem* 76(6):1201–1209.
11. Warmuth M, Kim S, Gu XJ, Xia G, Adrián F (2007) Ba/F3 cells and their use in kinase drug discovery. *Curr Opin Oncol* 19(1):55–60.
12. Whittaker S, et al. (2010) Gatekeeper mutations mediate resistance to BRAF-targeted therapies. *Sci Transl Med* 2(35):35ra41.
13. Wan PT, et al.; Cancer Genome Project (2004) Mechanism of activation of the RAF-ERK signaling pathway by oncogenic mutations of B-RAF. *Cell* 116(6):855–867.
14. Brennan DF, et al. (2011) A Raf-induced allosteric transition of KSR stimulates phosphorylation of MEK. *Nature* 472(7343):366–369.
15. McKay MM, Ritt DA, Morrison DK (2011) RAF inhibitor-induced KSR1/B-RAF binding and its effects on ERK cascade signaling. *Curr Biol* 21(7):563–568.
16. Hu J, et al. (2011) Mutation that blocks ATP binding creates a pseudokinase stabilizing the scaffolding function of kinase suppressor of Ras, CRAF and BRAF. *Proc Natl Acad Sci USA* 108(15):6067–6072.
17. Kaul A, Chen YH, Emnett RJ, Dahiya S, Gutmann DH (2012) Pediatric glioma-associated KIAA1549:BRAF expression regulates neuroglial cell growth in a cell type-specific and mTOR-dependent manner. *Genes Dev* 26(23):2561–2566.
18. Baljuls A, et al. (2011) Single substitution within the RKTR motif impairs kinase activity but promotes dimerization of RAF kinase. *J Biol Chem* 286(18):16491–16503.
19. Poulikakos PI, et al. (2011) RAF inhibitor resistance is mediated by dimerization of aberrantly spliced BRAF(V600E). *Nature* 480(7377):387–390.
20. Rajakulendran T, Sahmi M, Lefrançois M, Sicheri F, Therrien M (2009) A dimerization-dependent mechanism drives RAF catalytic activation. *Nature* 461(7263):542–545.
21. Joseph EW, et al. (2010) The RAF inhibitor PLX4032 inhibits ERK signaling and tumor cell proliferation in a V600E BRAF-selective manner. *Proc Natl Acad Sci USA* 107(33):14903–14908.
22. Heidorn SJ, et al. (2010) Kinase-dead BRAF and oncogenic RAS cooperate to drive tumor progression through CRAF. *Cell* 140(2):209–221.
23. Long GV, et al. (2012) Dabrafenib in patients with Val600Glu or Val600Lys BRAF-mutant melanoma metastatic to the brain (BREAK-MB): A multicentre, open-label, phase 2 trial. *Lancet Oncol* 13(11):1087–1095.
24. Ciampi R, et al. (2005) Oncogenic AKAP9-BRAF fusion is a novel mechanism of MAPK pathway activation in thyroid cancer. *J Clin Invest* 115(1):94–101.
25. Palanisamy N, et al. (2010) Rearrangements of the RAF kinase pathway in prostate cancer, gastric cancer and melanoma. *Nat Med* 16(7):793–798.
26. Raabe EH, et al. (2011) BRAF activation induces transformation and then senescence in human neural stem cells: A pilocytic astrocytoma model. *Clin Cancer Res* 17(11):3590–3599.